

Characterization of a soft magnetic catheter controlled by a permanent magnet

Mohammad Hasan Dad Ansari^{1,2,3}, Xuan Thao Ha^{1,2,3}, Dr. Mouloud Ourak³, Dr. Veronica Iacovacci^{1,2}, Dr. Gianni Borghesan³, Prof. Dr. Emmanuel Vander Poorten³ and Prof. Dr. Arianna Menciassi^{1,2}

¹ The BioRobotics Institute, Scuola Superiore Sant'Anna, Pisa 56025, Italy

² Department of Excellence in Robotics & AI, Scuola Superiore Sant'Anna, Pisa 56025, Italy

³ Robot-Assisted Surgery Group, Department of Mechanical Engineering, KU Leuven, Leuven 3001, Belgium
hasan.mohammad@santannapisa.it, hasan.mohammad@kuleuven.be

Abstract

Endovascular catheterization, an increasingly popular procedure, remains an arduous task due to the difficulty in controlling the bending of the catheter tips used in the procedure. One way to overcome this challenge is to use magnetic fields and gradients to manipulate a magnetic catheter tip remotely. In this paper, the response of a custom built magnetic soft catheter tip is investigated in terms of its bending when actuated with an external permanent magnet. The bandwidth of the catheter tip and its response with respect to the speed of external permanent magnet movement is reported. An ideal working area on the bending angle vs magnet distance hysteresis curve is also proposed.

1 Introduction

Endovascular interventions using catheters are becoming increasingly common to access deep and remote anatomic regions through the body lumens for clinical procedures [1]. Such catheters remain difficult to use in tortuous paths as the medical doctor is only able to control their pushing and twisting [2]. Remote actuation through magnetic fields generated outside the body could help in performing complex coordinated motion in three-dimensional (3D) space, as magnetic fields are safe and highly controllable [3]. Moreover, while bending and actuating traditional stiff catheters is problematic, soft bodied catheters can provide improved navigation even at acute angles. In fact, their soft nature could offer excellent possibilities to reduce injury-related complications [4]. In this study, a soft magnetic catheter tip is actuated using an external permanent magnet (EPM) to investigate its bending response. The study aims to investigate catheter tip bending response when varying its distance from the EPM, intended for bending control.

2 Experimental test system

The experimental setup is shown in Figure 1. A soft magnetic catheter tip was clamped on a horizontal surface and an EPM was brought closer to it as shown in Figure 1. The EPM was mounted on a vertical rail so that it could be manually moved up and down. The bending of the catheter was captured using an optical camera and a fiber Bragg grating (FBG) shape sensing fibre. Optical markers, placed on the EPM and on the catheter tip, were tracked to gauge the distance between the catheter tip and the EPM.

2.1 Materials and Methods

2.1.1 Catheter tip

The developed magnetic catheter tip is composed of a soft polymer embedded with NdFeB magnetic particles (5 μm diameter). It is 7cm in length. 2.3 mm in diameter, it is hollow, and it hosts an internal lumen of 0.9 mm. It is attached to a 4 Fr catheter so that the entire assembly can carry a guidewire within it. The magnetic particles give the catheter tip a distributed axial magnetization.

2.1.2 Actuating external permanent magnet

The EPM is cylindrical in shape (7 cm in length and 6 cm in diameter), diametrically magnetised with a 1cm through hole along its axis which is used for fixing to supporting structures.

2.1.3 Optical tracking

Custom-made optical markers containing three reflective fiducials were 3d printed. One such optical marker each was placed on the catheter base and on the EPM. An At-racsys® fusionTrack™ tracking system was set up to capture the distance between the two. The optical tracking system also tracks the orientation of the markers which helps in aligning the EPM with the catheter as shown in Figure 1.

2.1.4 Shape sensing

To capture and validate the different aspects of the catheter bending, a Prosilica® camera is placed alongside the catheter, and a multicore fiber Bragg grating (FBG) shape sensing fibre (FBGS®) is placed inside the catheter.

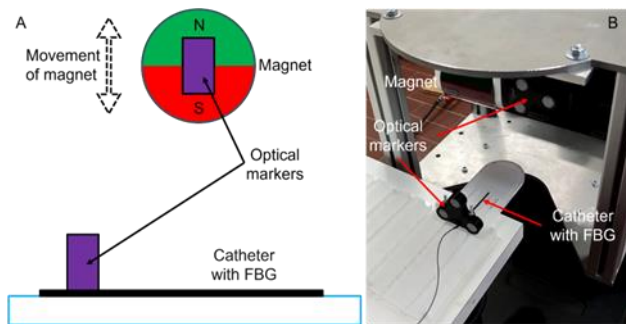


Figure 1: The benchtop experimental system used for the study. The EPM, catheter with FBG and the optical markers can be seen. A) A schematic diagram of side view and B) an image showing an isometric view of the experimental setup. The camera is placed outside the image frame capturing the side view of the catheter.

2.2 Experimental methodology

When the EPM is brought close to the catheter, the magnetic field and magnetic gradient acting on the catheter increase. The magnetic field brings the catheter to align its axis with the magnetic dipole of the EPM, while the magnetic gradient pulls the catheter towards it, thus bending the catheter tip. All data streams from the fusion-Track, the FBG, and the camera are synchronised and captured via ROS [5]. The bending angle derived from post-processing of data from the FBG is plotted against the distance of the EPM from the catheter and the resulting graph is shown in Figure 2.

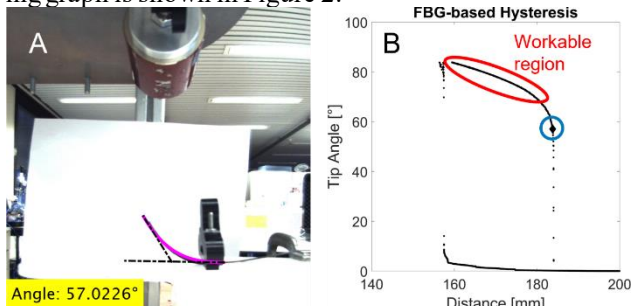


Figure 2: (A) FBG-based shape reconstruction of the catheter tip, which is drawn and superimposed on its captured image in magenta colour (left). The tip angle is measured by drawing a tangent at the tip; (B) the resulting tip angle vs distance hysteresis curve is plotted on the right with the workable region of the curve highlighted. The image in (A) corresponds to the point marked on the graph with a crossed diamond and circled in blue.

3 Results and discussions

The bending angle as observed from FBG, and the EPM distance as observed from the optical markers is plotted against each other to generate a hysteresis curve (Figure 2). As the EPM is brought closer to the catheter tip, it is found that the bending angle doesn't increase considerably until it reaches a point where the jump is sudden from near 0° to near 90° . This jump occurs when the distance between the EPM and the catheter tip is 15 cm.

This behaviour can be understood when considering the distribution of magnetic fields and gradients around the EPM. As reported in literature [6], a cylindrical permanent magnet can be approximated as a magnetic point dipole when the working space is beyond the radius of its minimum bounding sphere. In our case, the radius of the minimum bounding sphere is 4.6 cm. Since we do not work closer than that, we can assume the EPM to be a point dipole for the purpose of calculating the fields at a point in space, which is given by the equation:

$$\mathbf{B}(\mathbf{r}) = \frac{\mu_0}{4\pi} \left[\frac{3\mathbf{r}(\mathbf{m} \cdot \mathbf{r})}{r^5} - \frac{\mathbf{m}}{r^3} \right]$$

where μ_0 is the vacuum permeability constant, \mathbf{B} is the magnetic flux density, \mathbf{r} is the position vector of the point in space, and \mathbf{m} is the magnetic moment of the point dipole. This equation gives us the magnitude and the direction of the magnetic field around the EPM which is visualized in Figure 3. The magnetic field is visualised around the EPM in a cross-sectional plane perpendicular to its cylindrical axis since this is the working plane. The EPM is represented as a circle, its magnetization direction is represented by an arrow inside it, and the magnetic field around it is represented by the arrows in space. The direction of the arrows represents the direction of the field at that point and the length of the arrows represents the magnitude of the field with respect to each other.

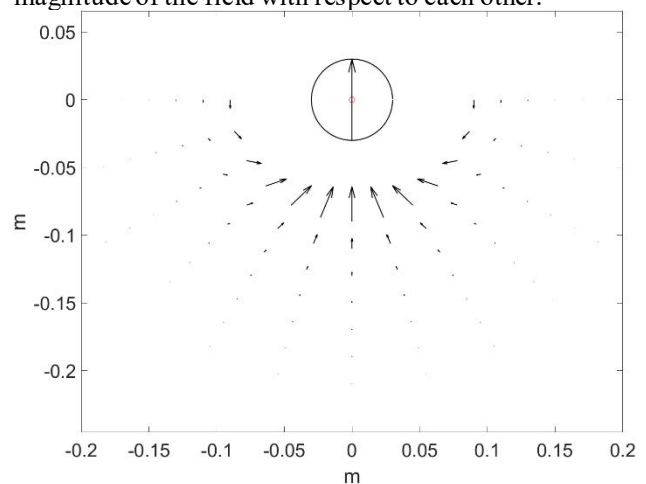


Figure 3: The magnetic field visualised around the EPM in a cross-sectional plane perpendicular to its cylindrical axis.

As can be seen that the magnitude of the magnetic field drops considerably with distance from the EPM. Not only the field magnitude but the field gradient magnitude too increases considerably when getting closer to the EPM. Both of these affect the catheter as the magnetic field applies a torque on the catheter tip to align it with itself, and the magnetic field gradient pulls the catheter tip towards the EPM. When the catheter tip is lying flat on a surface below the EPM, it resists bending due to gravity until the fields become strong enough to bend it. Once the catheter starts bending towards the EPM, it starts getting into the region of higher fields and higher gradients. Both of these further help the catheter to bend more which takes it to the region of even higher fields and gradients. Therefore,

this acts like a domino effect and the process stops when the catheter has reached its maximum bending angle which is 90°.

After reaching the maximum bending angle of the catheter tip, when the EPM is moved away, the reduction in bending angle is less sudden. That is because of the new shape of the catheter tip which is now aligned with the EPM magnetization and as a result much closer to the EPM. Even as the EPM is moved away, the catheter still is relatively close to the EPM resulting in a gradual decrease in the bending angle. This happens until the fields and gradients are not strong enough to overcome gravity in which case, the catheter tip starts falling down. As this happens, the catheter tip reaches regions with lower and lower fields and gradients, and therefore a sudden drop.

A representative hysteresis curve generated through such an experimental test shows an area, as highlighted in Figure 2, that appears ideal for controllable use of the catheter. In other words, the catheter tip is more controllable as long as its axis is aligned with the magnetization of the EPM, and the distance is not too big. The behaviour shown in Figure 2 was observed when the EPM was manually brought closer to the catheter tip as slow as possible, to eliminate any dynamic behaviour. Even in this case, the catheter bending was quite sudden and therefore it can be said that the catheter tip shows a high bandwidth and can respond to changes quickly.

We also investigated the catheter behaviour when the EPM was brought closer to the catheter tip as fast as possible (Figure 4). The hysteresis curve followed a similar behaviour where there are sudden jumps in the bending angle of the catheter tip both when the EPM is coming closer and when it is going farther. Moreover, the catheter tip also shows some oscillations before settling down at a stable bending angle. This is because of the dynamic effects of the catheter tip moving too fast.

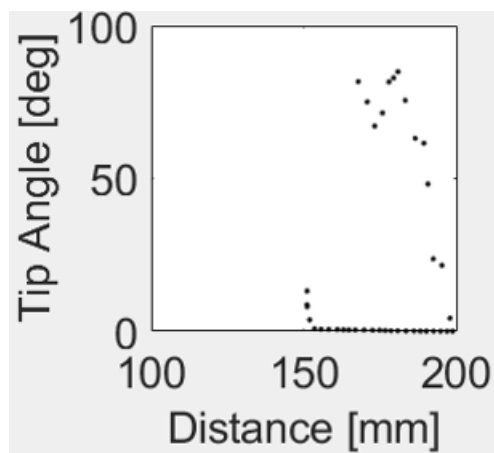


Figure 4: The resulting tip angle vs distance hysteresis curve when the speed of the EPM is as high as manually possible.

4 Conclusion and future work

A hollow hard-magnetic soft catheter tip was fabricated, and its bending angle was characterized against its distance from an EPM. This distance was tracked using an optical tracker, and the bending of the catheter tip was estimated using an FBG fibre inside it. The bending was also recorded using a camera and all three sensors were synchronised for data recording. The hysteresis curves between bending angle of the catheter tip and the distance of the EPM from it were plotted at different speeds of the EPM. It was found that the catheter tip has a high bandwidth and shows fast jumps in bending angle. Regions where the catheter tip is controllable have also been highlighted and proposed as the workable regions. In the future, this workable region could be exploited for a better control of the bending of the catheter tip. The EPM could always be placed at 15cm from the catheter tip and its magnetization always aligned with the axis of the catheter tip. For bending, the EPM can be moved in an arch of 15cm around the catheter tip while rotating the EPM such that the magnetization is aligned with the catheter tip axis.

Acknowledgement

This work was supported by the ATLAS project. The ATLAS project has received funding from the European Union's Horizon 2020 research and innovation programme under the Marie Skłodowska-Curie grant agreement No 813782.

5 Literature

- [1] D. Guez, D.R. Hansberry, C.F. Gonsalves, D.J. Eschelmann, L. Parker, and V.M. Rao; *Recent trends in endovascular and surgical treatment of peripheral arterial disease in the medicare population*, Journal of Vascular Surgery; vol. 71, pp. 2178, 2020.
- [2] M. Li, R. Obregon; J. J. Heit; A. Norbash; E. W. Hawkes; and T. K. Morimoto; *VINE Catheter for Endovascular Surgery*; in IEEE Transactions on Medical Robotics and Bionics; vol. 3; pp. 384-391, 2021.
- [3] F. Carpi, and C. Pappone; *Stereotaxis Niobe® magnetic navigation system for endocardial catheter ablation and gastrointestinal capsule endoscopy*, Expert Review of Medical Devices; vol. 6, pp. 487-498, 2009.
- [4] S. Gunduz, H. Albadawi, R. Oklu; *Robotic Devices for Minimally Invasive Endovascular Interventions: A New Dawn for Interventional Radiology*, Advanced Intelligent Systems; vol. 3, pp. 2000181, 2021.
- [5] M. Quigley, B. Gerkey, K. Conley, J. Faust, T. Foote, J. Leibs, E. Berger, R. Wheeler, A. Ng; *ROS: an open-source Robotic Operating System*, in ICRA workshop on open source software; vol. 3, pp. 5, 2009.
- [6] J. J. Petruska, J. J. Abbott; *Optimal permanent-magnet geometries for dipole field approximation*. IEEE transactions on magnetics 49.2: 811-819, 2012.